

26. Andreev, M. V., Drobakhin, O. O., Privalov, Y. N., Saltykov, D. Y. (2014). Measurement of dielectric material properties using coupled biconical resonators. *Telecommunications and Radio Engineering*, 73 (11), 1017–1032. doi: <https://doi.org/10.1615/telecomradeng.v73.i11.70>
27. Dyadenko, M. V., Gelai, A. I. (2017). Radio-Transparent Materials Based on Titanium Silicate Glass. *Glass and Ceramics*, 74 (7-8), 273–277. doi: <https://doi.org/10.1007/s10717-017-9978-0>
28. Yurov, V. M., Portnov, V. S., Puzeeva, M. P., Sadchikov, A. V., Orazbaeva, Zh. M. (2017). Some questions mechanical properties of nanoparticles and nanomaterials. *Fundamental research*, 12 (2), 349–353.

This paper proposes a technique to prevent the corrosion of steel reinforcement in concrete based on slag cement (SC) activated by Na(K) salts of strong acids (SSA) in the composition of by-pass cement kiln dust (BP). The technique implies using additional modifiers in the form of the Portland cement CEM I 42,5 R and the calcium-aluminate admixture (CAA) $C_3A \cdot 6H_2O$.

It is shown that adding the Portland cement contributes to enhancing the intensifying influence of BP on the SC hydration, accompanied by an increase in the strength of artificial stone. This effect is predetermined by the formation of hydrosilicates in hydration products with an increased crystallization degree in the form of CSH(I) and $C_2SH(A)$.

Modifying SC with CAA ensures the intensive formation of low-soluble AFm phases in the composition of hydration products, aimed at reliable binding the SSA anions (Cl^- , SO_4^{2-}) that are aggressive to steel reinforcement.

The study result has established the possibility to produce SC, activated by SSA, when using BP, the Portland cement, and CAA. Mathematical methods to plan the experiment were applied to produce an SC composition of "granulated blast furnace slag – BP – Portland cement – CAA", characterized by a strength class of 42.5 and a molar ratio of Cl^-/OH^- in a porous solution not exceeding 0.6. The resulting properties predetermine the feasibility of using SC in steel-reinforced concrete.

The relevance of this work is due to the modern trends in the development of the construction industry. The introduction of cement that contains mineral additives, in particular granulated blast furnace slag, contributes to improving the environment by reducing CO_2 emission. The use of such cement as a base of steel-reinforced concrete ensures the increase in their functionality and durability

Keywords: slag cement, steel reinforcement, cement kiln dust, AFm phase, structure formation

UDC 691.5: 691.3

DOI: 10.15587/1729-4061.2020.217002

DESIGN OF SLAG CEMENT, ACTIVATED BY Na (K) SALTS OF STRONG ACIDS, FOR CONCRETE REINFORCED WITH STEEL FITTINGS

P. Kryvenko

Doctor of Technical Sciences, Professor*

E-mail: pavlo.kryvenko@gmail.com

I. Rudenko

PhD, Senior Researcher*

E-mail: igor.i.rudenko@gmail.com

O. Konstantynovskiy

PhD, Associate Professor

Department of Building Constructions and Products**

E-mail: alexandrkp@gmail.com

*Scientific-Research Institute for

Binders and Materials**

**Kyiv National University of

Construction and Architecture

Povitroflotskyi ave., 31, Kyiv, Ukraine, 03037

Received date 30.09.2020

Accepted date 01.12.2020

Published date 03.12.2020

Copyright © 2020, P. Kryvenko, I. Rudenko, O. Konstantynovskiy

This is an open access article under the CC BY license

(<http://creativecommons.org/licenses/by/4.0>)

1. Introduction

Current trends in the development of the construction industry predetermine the relevance of introducing the so-called "green" materials whose production involves resource- and energy-saving technologies [1] implying a responsible attitude towards the environment [2]. The types of cement containing mineral additives of artificial and natural origin fully match the trends of sustainable development of mankind [3]. As regards the environmental aspect, replacing part of the clinker in cement composition with mineral additives contributes to reduc-

ing the emission of CO_2 [4]. At the same time, materials based on such types of cement are characterized by high quality, functionality, and durability. Thus, paper [5] shows the effectiveness of the use of multicomponent types of cement based on slag, zeolite, and fly ash in mortars by a high early strength [5]. The positive effect on the strength of concrete under various humid conditions of operation is exerted by admixtures of polydisperse zeolite tuff and perlite [6]. Applying admixtures in the form of zeolite or highly dispersed chalk in cement composition leads to an increase in strength indicators [7], crack resistance [8], and frost resistance of concrete [9].

Granulated blast furnace slag (hereinafter referred to as GBFS) as a component of cement is most effectively activated by hydroxides and salts of alkali metals, which enable alkaline reaction of the aqueous medium at high concentration [10]. That forms a binding system known as the alkaline-activated slag cement. The alkaline activation of aluminosilicate raw materials is widely used in the production of modern building materials [11]. Concrete based on the alkaline-activated types of cement is characterized by the increased indicators of strength [12], heat resistance [13], corrosion resistance [14], sulfate resistance [15], frost resistance [16], water resistance [17], compared to analogs based on conventional clinker concrete. Along with the high performance properties, the alkaline-activated slag cement can be used as a base of decorative materials [18]. There are data on the effective disposal of radioactive waste [19], as well as wastewater [20], when making safe building materials based on the alkali-activated types of cement. The principles were proposed for the reasonable selection of modifying admixtures for different functional purposes for concrete based on the alkaline-activated types of cement (plasticizers [21], redispersion polymeric powders [22], aimed at reducing the deformities of shrinkage [23], expandable admixtures [24]). This explains the widespread use of the alkaline-activated slag types of cement in modern concrete and mortars.

At the same time, it is known that, in addition to substances that provide for a high pH value of the medium, GBFS can also be activated by weakly-alkaline [25] and almost neutral salts [26].

It is a relevant task to improve the efficiency of using, in the role of activators of the slag types of cement (hereinafter referred to as SC), the Na(K) salts of strong acids (hereinafter referred to as SSA), formed by strong alkalis (for example, NaOH or KOH) and strong acids. The technical advantages of this type of activation include the reduced alkalinity of a binder, the minimized risk of working with highly-alkaline materials, the cement manufacturability compared to purely alkaline-activated analogs [27]. The SC that are activated by SSA are also applicable as specialized binders for the encapsulation of radioactive metals [26] and nuclear waste [28, 29].

Study [30] reported a mixed "alkaline-sulphate" type of activating the GBFS in cement composition. This technique involves the use of SSA together with compounds of alkalic metals, which are traditionally applied as alkaline activators [10]. This technique, first, provides for the relatively high pH values of the hydration environment, which ensures the preservation of the passive state of steel reinforcement. Second, favorable conditions are created for the formation of a larger Aft phase in the form of small-crystal ettringite. This fact determines the increase in cement strength, including early, the decrease in shrinkage deformations, and, consequently contributes to the durability of artificial stone.

An available source of SSA on an industrial scale is cement kiln dust (hereinafter referred to as BP), which forms in cement kilns when some of the gases rich in the salts of alkaline metals are released. This operation helps prevent the formation of a coating on kiln walls and reduce the content of compounds of alkaline metals in the clinker [31]. Typically, BP contains volatile substances such as sulfates and alkaline metals chlorides, raw material residues, and, partially, fired clinker [32]. A characteristic ingredient of BP is also free calcium oxide (CaO). BP aqueous extracts are characterized by high hydrogen indicator values (pH=13...14), which is a

prerequisite to use BP to activate GBFS in cement composition. In addition, there is a known benefit associated with the reduction of shrinkage deformations of SC when using, in addition to the alkaline activator, both BP [33] and SSA, which are the predominant ingredients of BP [34].

Consequently, the use of BP, which is a large-ton byproduct of the cement industry, as a source of SSA to improve the hydration activity of GBFS is a promising way of developing the construction industry, predetermined by a series of factors such as increasing the content of alkalic metal oxides in the Portland types of cement; transition to a dry production technique of the Portland cement clinker; using fillers containing active silica.

However, there are also shortcomings related to the slow hardening and insufficient strength of SC activated by SSA [27]. Paper [35] shows that the insufficient slag reaction capacity causes a corresponding reduction in the cement hydration products.

As a result, the required properties of SC are achieved only when using, as a base, a purely alkaline activator with the introduction of SSA in the form of, for example, sodium sulfate [36], or when using BP [37].

The above limits the market adoption and industrial application of the SC activated by SSA [27].

Thus, despite the validity of using SSA, including as part of BP, to activate the SC, there is an issue related to insufficient strength of the latter. This task is resolved by the additional involvement of activators in the form of "classical" compounds of alkaline metals. However, in this case, the very idea is compromised to use SSA to activate GBFS in order to ensure its respective technical advantages and set adequate market price for SC.

In addition, employing an SSA activating function in the form of chlorides and sulfates, in particular when using BP, limits the possibility of using CP in the steel-reinforced concrete. According to [38], there are two main processes that are combined during a corrosion attack on the steel reinforcement in concrete: a carbonation reaction and a spot (pitting) corrosion caused by chloride-ions. In turn, although sulfate-ions do not lead to the direct passivation of steel but determine the formation of hydrogen sulfide (H₂S), and are catalysts for the process of oxidation (carbonation) of hydrate new formations.

Consequently, the use of SSA, which, for example, are included in BP composition, to activate SC is related to the need to ensure sufficient strength of such cement. Another problematic issue is to counter the aggressive effects of the anionic residue of strong acids on steel reinforcement in concrete.

2. Literature review and problem statement

Doubts on the feasibility of solving the issue of SC strength by increasing the concentration of SSA are reasonably expressed in work [39]. It shows that the SSA concentration, such as Na₂SO₄, does not cause significant changes in the phase composition of hydrate new formations although it can affect the reactive capacity of slag [29]. In confirmation, study [40] demonstrates that the hardening of SC activated with Na₂SO₄ proceeds even faster than that of the analog activated by Na₂CO₃, and, accordingly, possessing a much higher pH value. However, the hardening of SC activated with the specified salts in any case requires

more time than when using sodium silicates. This can be explained by the fact that, first, the high content of alkaline metal compounds does not necessarily define the high pH values of a porous solution, as, for example, it is emphasized in work [39]. Second, sodium silicates are characterized by greater activation capacity relative to GBFS [41].

A different approach, and a more effective one according to [42], implies, rather than increasing the concentration of SSA, increasing the thinness of the grinding of the slag component of cement. This technique could improve the strength of SC, including early, without increasing the pH values. However, increasing the fraction of GBFS grinding could become an unnecessarily energy-consuming and economically inappropriate way to increase the SC strength [43].

An alternative worth considering is the activation of GBFS not only by the compounds of alkali metals. Thus, the authors of [39] indicate that the strength of SC depends primarily on the content of reactive phases, including lime and clinker phases, if BP is to be a source of SSA. This is confirmed by the formation of calcium hydroaluminates and hydrosilicates in the hydration products of the SSA-activated SC based on BP. Work [42] also reported the phases of low-base CSH (I) calcium hydrosilicates as the basic hydration products of SC activated by SSA. Studies [44, 45] note that the issue related to low cement strength is associated with a low Ca/Si ratio in the specified phases. The expediency of an additional calcium activation of slag in the composition of the alkaline-activated SC was confirmed as a way to improve strength when using the additives of lime [46] or the Portland cement [34].

As regards resolving the issue of counteracting the aggressive influence of the anionic residue of SSA (Cl^- , SO_4^{2-}) on steel reinforcement, work [47] demonstrates the greater impact of GBFS on the binding capacity of the system than that of the clinker component. It is shown that when the content of the slag component increases, the concentration of free chlorine decreases while the value of the critical chlorine content (C_{crit}) increases. That indicates that the content of Cl^- ions, bound in *AFm* phases, is higher than the amount absorbed by calcium hydrosilicates. Study [48] explains that when the content of the slag component in SC increases, the formation of *AFm* phases increases because it is associated with an Al_2O_3 content in the system.

Within the context of the impact of the composition of SC hydration products on the binding of the anionic component of SSA, paper [42] revealed the formation of a significant volume of *Aft* phase in the form of ettringite. One would assume that this phase is crucial not only for resolving the issue of SC strength, especially at an early age, but also for determining the chemical binding of free anions of SO_4^{2-} , Cl^- , CO_3^{2-} , etc. However, life is not that simple. Thus, on the one hand, the ability to bind Cl^- ions by such phases gradually decreases with an increase in the content of SO_4^{2-} ions as shown in work [48]. This effect is explained in work [49] by the fact that sulfate reduces the binding of chlorine in the C-S-H and *AFm* phases. This is due to the ability of hydrosilicates to replace chlorine ions with sulfate-ions and a partial conversion of *AFm* phases into *Aft* phases (ettringite). On the other hand, paper [50] revealed a larger stabilization of the *AFm* phase ($\text{Al}_2\text{O}_3\text{-Fe}_2\text{O}_3\text{-mono}$) compared to ettringite due to the increased hydration medium alkalinity.

In this regard, the result reported in [51] is promising; it shows that the amount of bound chlorine (P_{cb}) depends

on the type of the activator, the W/C value, and the content of phases the type of C-S-H. Second, this indicator depends on the content of the starting phases of C_3A and C_4AF , from which the *AFm* phases form, including Friedel salt ($3\text{CaO}\cdot\text{Al}_2\text{O}_3\cdot\text{CaCl}_2\cdot 10\text{H}_2\text{O}$). The role of aluminum-containing phases in the hydration process is confirmed by the conclusions in [52], which shows that, for the case of an activator in the form of SSA, it is the slag component of cement that determines the additional ability to bind chlorine. The authors reasonably assumed that this is due to the transformation of the already formed ettringite (a phase of the *Aft* type) into phases of the *AFm* type. Ettringite and monosulfoaluminate are considered to be the basic hydration products of C_3A in paper [53]. That gives grounds for considering C_3A as a mineral additive for the modification of the SSA-activated SC based on BP.

It is also important to ensure a certain equilibrium within a binding system to enable the reliable binding of the anion part of SSA. As regards the diversity of *AFm* phases, work [54] shows that they may include different anions (Cl^- , SO_4^{2-} , CO_3^{2-} , OH^- etc.). Depending on that, the *AFm* phases could be represented by monocarboaluminate, hemicarboaluminate, strathlingite, hydroxy-*AFm* phase, monosulfoaluminate, etc. Work [55] shows the possibility of forming a nitrate *AFm* phase along with chloride and sulphate ones. At the same time, work [40] demonstrates the absence of ettringite and monosulfoaluminate in hydration products when Al_2O_3 is lacking, even with a sufficient content within the binding system of compounds of alkaline-earth metals. The confirmation of this thesis indicates that the lack of C_3A and C_4AF in the system is generally an obstacle to the condensation of Friedel salt [56].

Another problematic issue is ensuring the stability of phases already formed during hydration with the aggressive ions bound in them, engaged from SSA. For example, in *AFm* phases, it is possible to replace chlorine with carbonate groups, as described in work [57]. Another example is the results reported in [58], which show that the stability of bound chlorine is also sensitive to the action of SSA in the form of Na_2SO_4 . Under conditions of a sulfate attack, there is a risk of chlorine transition from a bound state into a free state in the bond and its substitution with a sulfate ion at Friedel salt decomposition. The monosulfoaluminate (*AFm* phase) that forms during an ion exchange between Cl^- and SO_4^{2-} , could then turn into ettringite (*Aft* phase). This, in turn, could cause the danger of secondary ettringite formation in artificial stone.

In this regard, study [59] shows that building mortars based on SC activated by $\text{Ca}(\text{OH})_2$ demonstrate higher corrosion resistance than the analogs that were activated, for example, by alkalis (KOH, NaOH). The authors associate it with the formation of an unstable phase of $\text{Ca}(\text{OCl})_2$ and the appropriate removal of free chlorine from the porous fluid. Given a known additional activation and the participation of the slag component in the creation of new formations capable of binding anions, the use of calcium additives to modify the SSA-activated SC is a promising way to stabilize hydrate new formations.

Consequently, our analysis of the scientific literature reveals the need to ensure that the SC activated by SSA should include the required content of starting phases and compounds involved in the formation of *Aft* and *AFm* phases in the products of new formations during hydration. This technique corresponds to modern approaches applied in materials scien-

ce [60] and is reasonable to counteract the aggressive effects of the anionic residue of strong acids on steel reinforcement in concrete. It could be assumed that the advantage in the formation of these phases would depend both on the composition and content of SSA and the composition (alkalinity) of the cement matrix, the morphology of hydrate new formations, and the transporting properties of the structure of concrete in general.

The generalization of the above results makes it possible to predict the prospects for using SSA to activate the hydraulic properties of GBFS to produce SC. In practical terms, BP could be considered as a source of SSA. It could be predicted that to ensure the strength of SC and its safe use in reinforced concrete, it is advisable to use modifiers. Such modifiers should provide additional calcium activation of GBFS and the formation of phases capable of reliable binding of SSA anions, aggressive against steel reinforcement. This renders relevance to investigating the SC activated by SSA in the BP composition as a base of the steel-reinforced concrete.

3. The aim and objectives of the study

The aim of this study is to devise an effective technique to prevent the corrosion of steel reinforcement in concrete based on SC, activated by SSA in the BP composition.

To accomplish the aim, the following tasks have been set:

- to investigate the impact of SSA in the BP composition on the activation of GBFS and the structure formation of SC;
- to examine the impact of the Portland cement admixture on the structure formation of SC activated by BP;
- to study the effectiveness of binding chlorine in the BP composition by a calcium-aluminate admixture (hereinafter referred to as CAA) to the *AFm* phase as part of the SC hydration products;
- to determine the optimal region of SC formulations for the composition “GBFS – BP – SC – CAA”, suitable for use in reinforced concrete, and to study patterns of their structure formation.

4. Materials and methods to study the effectiveness of using modifying admixtures in slag cement

4.1. Raw materials

We have used the following raw materials, typical of EU countries, as SC components:

- BP (CEMEX Zement GmbH, Rudersdorf, Germany), specific surface $S_{surf}=8,200 \text{ cm}^2/\text{g}$ (mineralogical composition: free calcium oxide (CaO), salts of alkaline metals and strong acids in the form of potassium chloride (KCl) and potassium sulfate (K_2SO_4), the complex compound of alkaline metals sulfates aphthitalite ($\text{K}_3\text{Na}(\text{SO}_4)_2$));
- GBFS (ThyssenKrupp Steel Europe AG, Dortmund, Germany), which belongs to a group of weak-acid (neutral) ones; specific surface $S_{surf}=3,860 \text{ cm}^2/\text{g}$ (by Blaine), basicity module $M_b < 1$, phase composition – fiberglass, represented by calcium aluminosilicates;
- a calcium-containing admixture – the Portland cement CEM I 42,5 R (hereinafter, PC) (Dyckerhoff GmbH, Wies-

baden, Germany) according to EN 197-1 (mineralogical composition, %: $\text{C}_3\text{S} - 42.3$, $\text{C}_2\text{S} - 28.6$, $\text{C}_3\text{A} - 8.8$, $\text{C}_4\text{AF} - 7.6$; – a structure-forming CAA to attract free chlorine (sulfate) to the *AFm* phase composition – a by-product of ettringite production in the form of hexahydrous tricalcium calcium aluminate ($\text{C}_3\text{A}\cdot 6\text{H}_2\text{O}$) (the content of $\text{C}_3\text{A}\cdot 6\text{H}_2\text{O}$ in the product composition is 86.07 %) (Knauf Gips KG, Iphofen, Germany).

The chemical composition of raw materials is given in Table 1.

Table 1

Chemical composition of raw materials

Raw materials	Oxide content, %										
	SiO ₂	Al ₂ O ₃	Fe ₂ O ₃	CaO	CaO _{free}	MgO	SO ₃	Na ₂ O	K ₂ O	Cl	TiO ₂
BP	9.1	2.8	1.7	27.1	10.1	0.9	12.0	1.3	24.9	14.3	–
GBFS	36.4	12.0	1.1	39.9	–	7.3	0.4	0.3	0.6	–	0.47
PC	21.1	4.9	2.5	63.1	2.1	1.5	3.2	0.2	1.2	0.1	0.19
CAA	–	23.2	–	44.4	–	–	0.1	–	–	0.007	–

The examined SC was prepared by the dry mixing of components.

Standard CEN sand according to EN 196-1 was used as a small filler in the study of strength evolution.

The solvent mixtures were mixed with water at the laboratory blade mixer HOBART.

4.2. Methods to study the effectiveness of modifying admixtures on the SC properties

The cement stone microstructure evolution was investigated by the following methods of physical-chemical analysis: differential-thermal (DTA) – at the derivatograph by R. Paulik, I. Paulik, L. Erdey made by IOM (Budapest, Hungary); probe analysis – at the raster electron microscope-microanalyzer REMMA 102-02 (made by OAO “SELMI”, Sumy, Ukraine).

In order to assess the degree of the chemical and adsorption binding of chlorine in BP by hydrate new formations, we performed a chemical analysis of the porous solution of hydrated samples of SC according to a procedure given in [61]. To carry out a chemical analysis of the porous fluid, the SC samples were mixed with distilled water at $\text{W/C}=0.5$. The resulting slurry was stored over the required period at a temperature of 20 °C in sealed plastic cylinders. Porous liquid was obtained by pressing at a maximum pressure of 375 MPa. The porous solution was taken during pressing into plastic flasks, which were then sealed. The chemical analysis of porous solutions was performed at the ISC-OES optical emission spectrometer.

Normal consistency of cement pastes (NC) and setting time were determined according to DSTU B V.2.7-185:2009.

The SC strength was determined using the samples of 40×40×160 mm, made from a cement-sand mortar (1:3) in accordance with DSTU B V.2.7-187.

The SC compositions were optimized by applying mathematical methods of planning the experiment.

5. The results of devising the formulation for slag cement activated by Na(K) salts of strong acids

5.1. The activation of granulated blast furnace slag by cement kiln dust

We have investigated the influence of BP content on the SC activity of the “GBFS – BP” composition in order to de-

termine the rational limits of BP content. According to the results in Fig. 1, the content of BP involved in the processes of structure formation increases with the extension of the hardening period of SC. Thus, on day 2 of hardening, the maximum activity is achieved at a BP content in the amount of 10.0 % by weight (hereinafter, %). This effect could be due to the time-stretched processes of interaction of SC components as a result of the high density of the aluminosilicate phase of the slag. In this regard, the role of BP as an SC intensifying component should be considered taking into consideration the time factor.

The patterns in the SC structure formation of the “GBFS – BP” composition, characterized by maximum strength, are investigated using DTA (Fig. 2), electron microscopy (Fig. 3, a, 4, a), and a probe analysis (Fig. 3, b, 4, b).

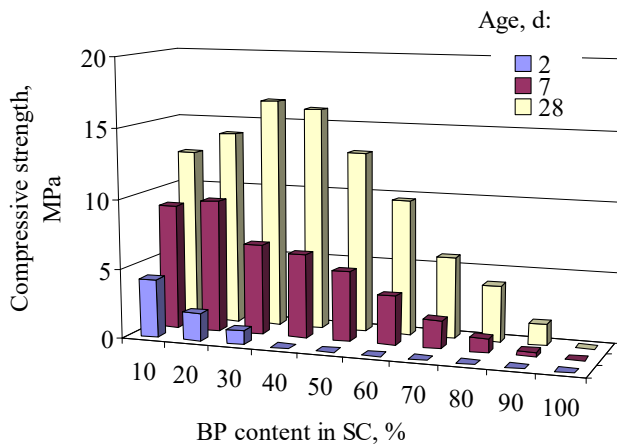


Fig. 1. Influence of BP content on the activity of SC of the “GBFS – BP” composition

According to DTA, the strength formation in the artificial stone of the hydrated SC of the “GBFS – BP” composition on day 2 of hardening is due to the formation of low-base calcium hydrosilicates of the structure CSH(I). The formation of these phases is due to the endoeffects at $t=165$ and 350 °C (dehydration) and exoeffect at $t=860$ °C (crystallization into wollastonite) (Fig. 2, curve 1).

The presence of *AFm* phases in the form of Friedel salt $3CaO \cdot Al_2O_3 \cdot CaCl_2 \cdot 10H_2O$ (endoeffect at $t=165$ °C – dehydration; exoeffect at $t=725$ °C – decomposition) and calcium hydrosulfoaluminate $3CaO \cdot Al_2O_3 \cdot CaSO_4 \cdot 12H_2O$ (endoeffect at $t=165$ °C – dehydration; exoeffect at $t=800$ °C) indicates the involvement of the ions of BP salts in the processes of structure formation. In addition, in the compositions of hydration products, we identified arcanite K_2SO_4 (endoeffect at $t=700$ °C – re-crystallization) and sylvite KCl (endoeffect at $t=745$ °C – melting). The presence of the specified salts in the phase composition of the hydrated stone indicates their insufficient involvement in the structure formation process, which adversely affects the activity of SC.

In addition to these phases, in the products of hydration we identified unbound portlandite $Ca(OH)_2$ (endoeffect at $t=565$ °C – dehydration and transition to CaO).

Hardening for 28 days is accompanied by an increase in the degree of crystallization of hydrosilicates CSH(I) and *AFm* phases (Friedel salt, calcium hydrosulfoaluminate), as evidenced by the displacement of the endo- and exoeffects towards the region of elevated temperatures (Fig. 2, curve 2).

An analysis of the electron microphotographs of an artificial stone chip’s surface and data from the probe analysis of

hydrated SC of the “GBFS – BP” composition confirms the creation of new formations identified by DTA (Fig. 3, 4). According to the probe analysis data (Fig. 3, b), we registered, on day 2 of hardening, in the SC hydration products the formation of the “embryos” of Friedel salt (content, %: $CaO - 35.14, Al_2O_3 - 18.34, Cl - 15.45$) and calcium hydrosulfoaluminate (content, %: $CaO - 37.28, Al_2O_3 - 15.72, SO_3 - 12.49$) in the form of needle-shaped new formations (Fig. 3, a). On day 28, there is a re-crystallization of the “embryos” into hexagonal thin-plate crystals of the *AFm* phases (Fig. 4, a, b).

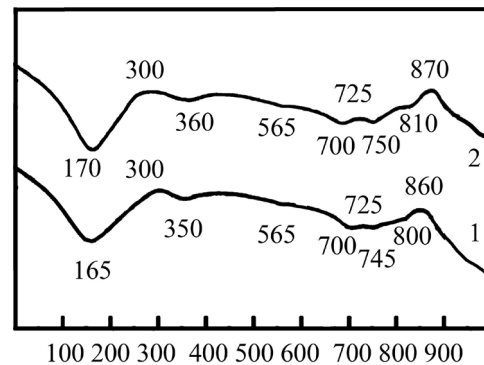
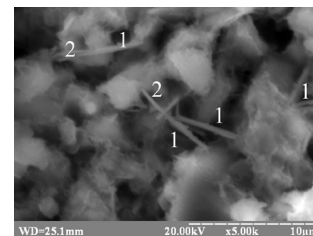
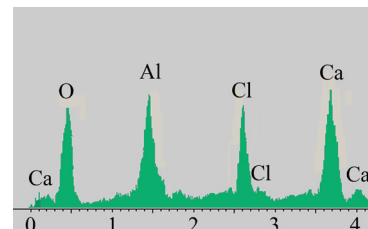


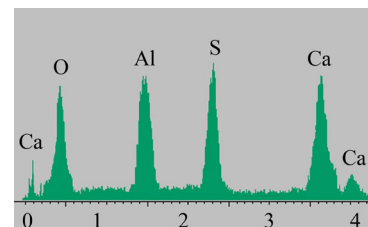
Fig. 2. The curves acquired from the differential-thermal analysis of SC of the “GBFS – BP” composition: 1 – on day of hardening; 2 – on day 28 of hardening



a



b



c

Fig. 3. Characteristics of the microstructure of SC of the “GBFS – BP” composition after 2 days of hardening: a – an electron microphotography of the chip’s surface; b, c – a probe analysis of the new formations, marked 1 and 2, respectively

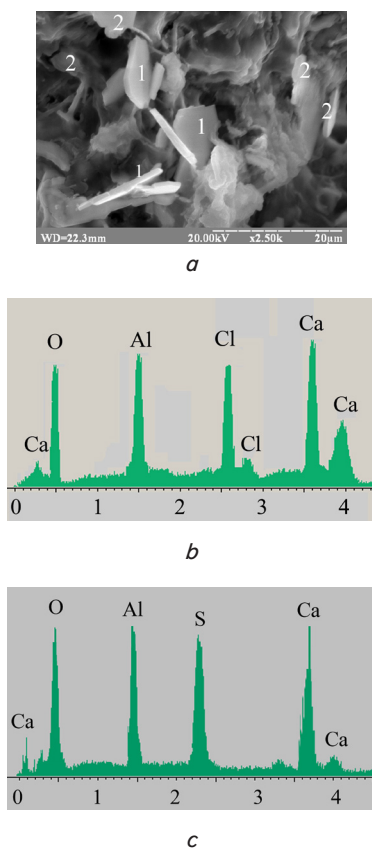


Fig. 4. Characteristics of the microstructure of SC of the “GBFS – BP” composition after 28 days of hardening: *a* – an electronic microphotograph of the chip’s surface; *b, c* – a probe analysis of the new formations, marked 1 and 2, respectively

According to the study results, there is an activation of the hydraulic properties of GBFS when using BP. We draw a conclusion about the possibility of using BP as an intensifying component for SC. The ratio of the components of SC of the “GBFS – BP” composition should satisfy the following condition: the ratio of alkaline metal oxide content (K_2O+Na_2O) in the BP composition to the content of aluminum oxide (Al_2O_3) in the GBFS composition should be $\frac{K_2O+Na_2O}{Al_2O_3} \geq 1$.

Table 2

Setting time of SC of the “GBFS – BP” composition

Component content, %		Setting time, hour – min	
GBFS	BP	start	finish
90.0	10.0	6–15	9–15
80.0	20.0	7–15	11–15
70.0	30.0	>12–00	>12–00
60.0	40.0	>12–00	>12–00

In this case, the low intensity of new formations’ creation in the initial hydration periods of SC determines the time-stretched hardening period (Table 2) and unacceptably low absolute values of strength (Fig. 1). This could be explained both by insufficient activity of the slag component of the SC and by the excess content of soluble salts (primarily chloride and potassium sulfate) in cement stone.

To improve the SC activity, the Portland cement (PC) admixture (PC) is involved in the system.

5.2. The structure formation of slag cement of the “granulated blast furnace slag – cement kiln dust – Portland cement” composition

We have investigated the impact of a PC additive on the strength of SC activated by SSA in the BP composition. The ratio of GBFS:BP in the SC composition ranged from 80:20 to 50:50. PC content varied from 11.0 to 17.0 %. The ratio of the components in the SC composition is given in Table 3.

It is determined that the maximum strength corresponding to class 32,5, in accordance with EN 197-1, is demonstrated by SC at a ratio of SC:BP of 80:20 (Fig. 5).

Our results determine the feasibility of the further search for the formulation solutions for SC towards reducing the content of PC from 17.0 to 7.5 % at a ratio of GBFS:BP of 80:20. To this end, the influence of the PC supplement on the terms of hardening (Table 4) and the SC strength (Fig. 6) was investigated.

Table 3

The ratio of components in SC of the “GBFS – BP – PC” composition

Component content, %			GBFS:BP ratio
GBFS	BP	PC	
66.0	17.0	17.0	80:20
59.0	26.0	15.0	70:30
52.0	35.0	13.0	60:40
45.0	44.0	11.0	50:50

Our results demonstrate the lack of proportional dependence of the SC activity on the content of PC. The greatest strength characterizes the SC with a PC content of 13.5 %, which corresponds to class 32.5: compression strength on day 2 and 28 is 9.6 and 29.1 MPa, respectively. It is obvious that the optimal ratio of components in SC determines its non-additive properties for strength. The analysis of the terms of hardening (Table 3) confirms this conclusion.

The methods of a physical-chemical analysis (Fig. 7–9) were applied to study the patterns of structure formation of SC of the “GBFS – BP – SC” composition, characterized by the greatest strength. According to the results from DTA, we identified in the products of SC hydration, on day 2 (Fig. 7, curve 1), the low-base calcium hydrosilicates of the structure CSH(I). This is confirmed by the endoeffects at $t=165$ and 350 °C (dehydration) and exoeffect at $t=860$ °C (re-crystallization into wollastonite). In addition, the formation of hydrosilicates of the $C_2SH(A)$ structure (endoeffects at 420 and 480 °C) was registered. Thus, the increase in the strength of SC of the “GBFS – BP – PC” composition, compared to the composition of “GBFS – BP”, is caused by a greater content of calcium hydrosilicates (CSH(I), $C_2SH(A)$) in the products of hydration.

In addition, we registered in the products of SC hydration Friedel salt (endoeffect at $t=165$ °C – dehydration; exoeffect at $t=725$ °C – decomposition) and calcium hydrosulfoaluminate (endoeffect at $t=165$ °C – dehydration; exoeffect at $t=800$ °C). The endoeffect at $t=565$ °C indicates the presence of the unbound portlandite $Ca(OH)_2$ in the system. The exoeffects at $t=700$ and 745 °C indicate the presence of salts in the hydration products that have not fully participated in

the structure formation of SC – arcanite K_2SO_4 and sylvite KCl , respectively.

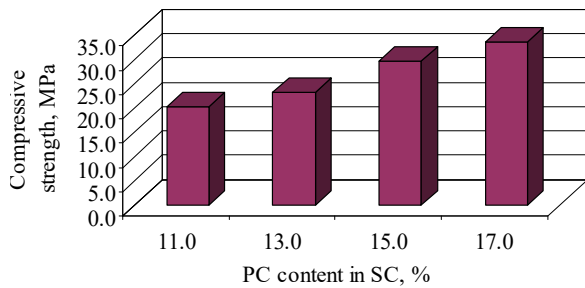


Fig. 5. The impact of PC on the strength of SC of the “GBFS – BP – PC” composition on day 28 of hardening

Table 4

Setting time of SC of the “GBFS – BP – PC” composition

Component content, %			NC, %	Setting time, hour – min	
GBFS	BP	PC		start	finish
66.0	17.0	17.0	28.5	5–10	7–30
69.0	17.5	13.5	3.5	5–05	7–15
71.0	18.0	11.0	31.0	5–35	7–45
74.0	18.5	7.5	31.5	7–00	10–30

On day 28 of SC hardening, we registered an increase in the degree of crystallization of hydrosilicates and *AFm* phases (Friedel salt, calcium hydrosulfoaluminate), which is confirmed by the displacement of the corresponding endo- and exoeffects towards the region of elevated temperatures (Fig. 7, curve 2).

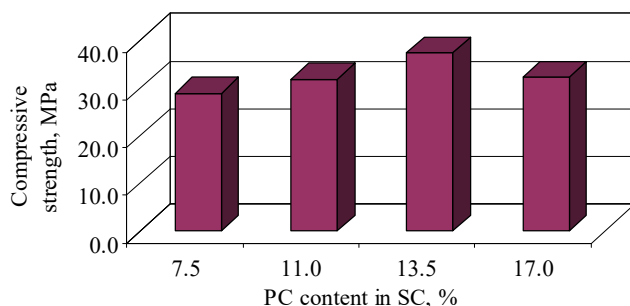


Fig. 6. Influence of PC content on the strength of SC of the “GBFS – BP – PC” composition on day 28 day of hardening

The electron microphotographs of the stone chip’s surface and the data from a probe analysis complement the idea of the structure formation of SC of the “GBFS – BP – PC” composition. Thus, the addition of PC admixture to the SC composition ensures the increased content of Friedel salt on day 2 in the form of the already formed hexagonal plates (Fig. 8, *a*). The formation of Friedel salt in the hydration products is confirmed by the probe analysis data (content, %: CaO – 37.23, Al_2O_3 – 19.87, Cl – 17.38) (Fig. 8, *b*). On day 28, there is a further crystallization of Friedel salt (content, %: CaO – 38.48, Al_2O_3 – 20.15, Cl – 18.57) and calcium hydrosulfoaluminate (content, %: CaO – 36.18, Al_2O_3 – 17.25, SO_3 – 18.57) in the form of clusters of hexagonal plates of a larger size (Fig. 9, *a, b*). DTA data confirm an increase in the degree of crystallization of *AFm* phases

when adding PC to the SC composition (Fig. 6). The explanation for such an evolution of the structure formation of SC may be the intensification of the involvement of portlandite $Ca(OH)_2$ in the composition of hydrate new formations.

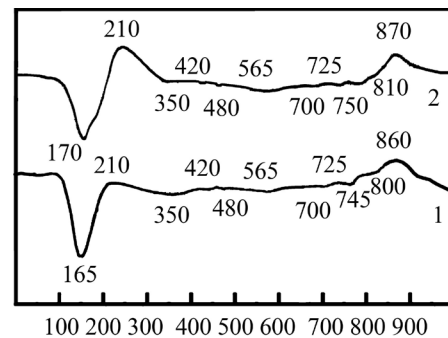
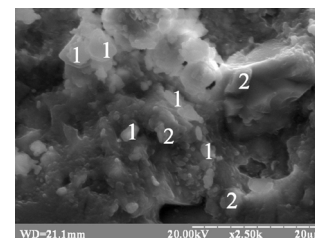
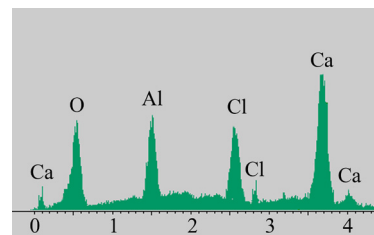


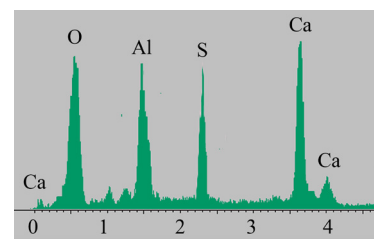
Fig. 7. The curves acquired from a differential-thermal analysis of SC of the “GBFS – BP – PC” composition: 1 – on day 2 of hardening; 2 – on day 28 of hardening



a



b



c

Fig. 8. Characteristics of the microstructure of SC of the “GBFS – BP – PC” composition after 2 days of hardening: *a* – electron microphotograph of the chip’s surface; *b, c* – a probe analysis of the new formations, marked 1 and 2, respectively

Thus, we have shown the possibility of producing SC when using BP as a source of SSA, which contributes to revealing the hidden hydraulic activity of GBFS and is a structure-forming component of the binding system. The use of an additional component in the form of PC provides for the reinforcement of the intensify-

ing influence of SSA on the slag component, accompanied by the formation of the SC required strength.

It is known that the main criteria for assessing the suitability of SC for use in steel-reinforced concrete include, in addition to activity, the content of free chlorine in a porous solution of hydrated SC. The content of chlorine-containing salts determines the need to substantiate BP in the SC composition, which ensures the preservation of the passive state of the reinforcement.

The absence of conditions for reinforcement depassivation is ensured at the molar ratio $Cl^-/OH^- \leq 0.6$ in the porous solution. However, the ratio of Cl^-/OH^- in the porous solution of hydrated SC of the “GBFS – BP – PC” composition is 9.83.

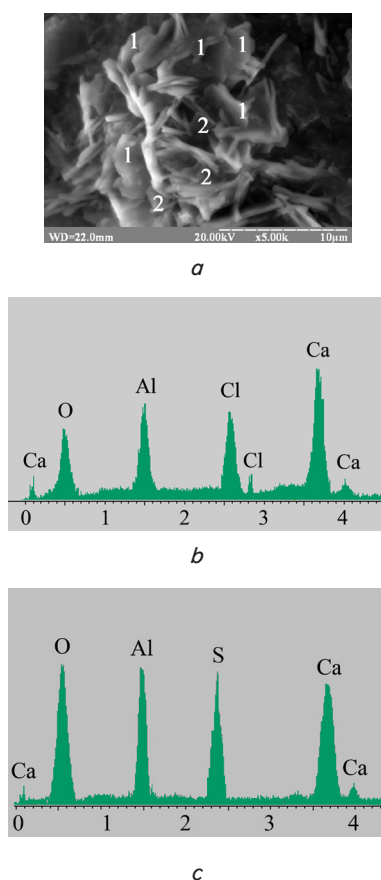


Fig. 9. Characteristics of the microstructure of SC of the “GBFS – BP – PC” composition after 28 days of hardening: *a* – electron microphotograph of the chip’s surface; *b*, *c* – a probe analysis of the new formations, marked 1 and 2, respectively

Reducing the content of free chlorine in an SC porous mortar is possible by its chemical or adsorption binding.

5. 3. The kinetics of Friedel salt formation when modifying slag cement by a calcium-aluminate admixture

For the accelerated formation of *AFm* phases, represented by the system of complex salts $3CaO \cdot Al_2O_3 \cdot CaSO_4 \cdot nH_2O$ -, $3CaO \cdot Al_2O_3 \cdot CaCl_2 \cdot 10H_2O$ -, $3CaO \cdot Al_2O_3 \cdot Ca(OH)_2 \cdot nH_2O$ -, we propose the introduction of CAA in the form of hexahydrated tricalcium calcium aluminate ($C_3A \cdot 6H_2O$). This substance is characterized by a much larger surface of molecules compared to single- and two- calcium aluminate, which

determines greater adsorption and, consequently, a greater degree of chlorine binding into Friedel salt.

We have investigated the effect of the Cl/Al molar ratio on the degree of chlorine binding as part of SC hydration products. The study was conducted on the model system “BP – CAA” (Table 5). In this system, BP determines the main content of chlorine, CAA – the main content of reactive (at the initial stage of hydration) alumina in the SC composition.

Table 5

Component content in the model system		Molar ratio Cl/Al
BP	CAA	
26.7	73.3	0.32
42.3	57.7	0.65
46.0	54.0	0.75
53.1	47.0	1

The results of our study after 7 days of hydration of the model systems are shown in Fig. 10. The results suggest that the optimal molar ratio is Cl/Al=1, which corresponds to the stoichiometric calculation of the Friedel salt formation reaction. This ratio between the Cl and Al ions corresponds to the content of 53.1 % of BP and 47.0 % of CAA in the model system’s composition (BP:CAA=1.13).

The low absolute values of the degree of binding of chlorine with a sufficient content of C_3A to implement the process are explained by the different crystallization kinetics of portlandite ($Ca(OH)_2$) and Friedel salt. Thus, the analysis of the BP heat production curve during hydration (Fig. 11) indicates the completion of the CaO transition to portlandite within the first 3 hours of hydration. The intensive formation of Friedel salt occurs during the first 4–5 days of hydration. Thus, in the formation of complex salts $3CaO \cdot Al_2O_3 \cdot CaCl_2 \cdot 10H_2O$ and $3CaO \cdot Al_2O_3 \cdot Ca(OH)_2 \cdot nH_2O$, the equilibrium shifts towards the formation of the latter. The high content of SO_4^{2-} ions determines the formation of H_2S and, consequently, the high intensity of system’s carbonation. This scheme of the process explains the slower formation of Friedel salt given a known priority of Cl^- ions over OH^- ions.

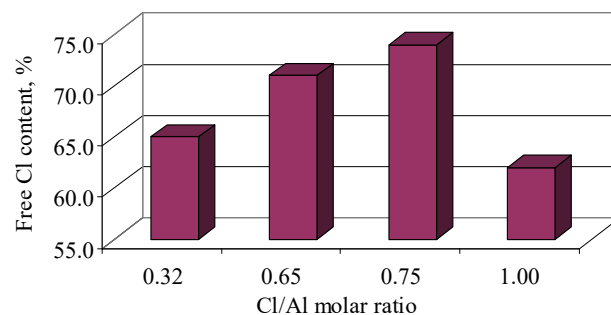


Fig. 10. Dependence of the degree of chlorine binding on the Cl/Al molar ratio during the hydration of the model system “BP – CAA”

The analysis of the Friedel salt formation kinetics in the model system under the influence of CO_2 from the air and in its absence (Fig. 12) confirms our results. The greatest intensity of Friedel salt formation was registered over the first 48 hours of hardening both in the absence of CO_2 influence (Fig. 12, *a*) and under its influence (Fig. 12, *b*).

However, while in the absence of CO₂ effect we observed salt formation during the entire period of hardening, then under the CO₂ influence most salt could form only during the initial stages of hardening. This is due to a significant slowdown in Friedel salt formation under conditions of influence exerted by CO₂ from the air, especially given the catalysis function of hydrogen sulfide (H₂S) in carbonation.

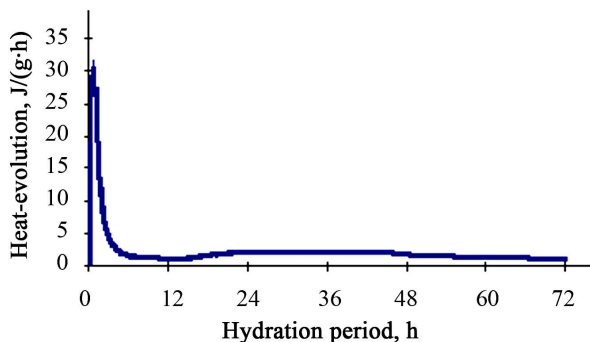


Fig. 11. Integrated heat-evolution during BP hydration

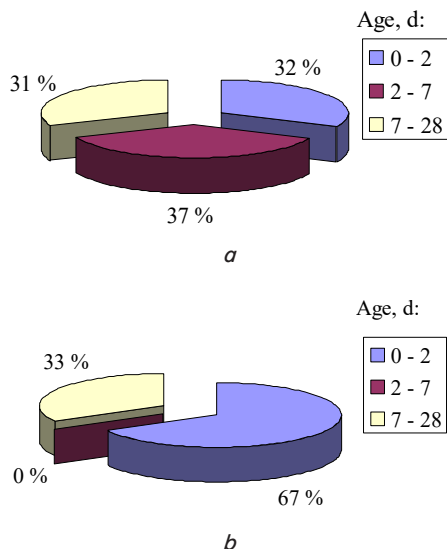


Fig. 12. The kinetics of Friedel salt formation over 28 days of hardening of the model system “BP – CAA” depending on the influence exerted by CO₂ from the air: a – without influence, b – under the influence

Consequently, the formation duration of portlandite Ca(OH)₂ in the hydration of the model system “BP – CAA” and its transition to calcite determine the intensity of Friedel salt formation under the influence of CO₂. Sealing the structure of the material when using surface-active substances (hereinafter referred to as SAS) that performing a water-reducing function is a solution to prevent the development of carbonization [62]. The use of organic compounds is a priority direction in the manufacturing technology of various building materials, both concrete and wood-based [63], reed-based [64] ones, etc.

The technique of compacting the structure of concrete is also the use of a complex of salts CaCl₂, NaNO₃, and Na₂SO₄, which helps increase the water resistance of the material by clogging the pores by the formed crystal hydrates [65].

The SC of the “GBFS – BP – PC – CAA” composition could be suggested as a base for reinforced concrete given its sufficiently high activity and the possibility of binding chlorine into Friedel salt. The SC activity is ensured by joint activation of GBFS with the BP and PC admixtures. Binding of chlorine into Friedel salt is implemented due to the modifying function of CAA.

5. 4. The structure formation of slag cement of the “granulated blast furnace slag – cement kiln dust – Portland cement – calcium-aluminate admixture” composition

By using a method of methodical planning of the experiment, we have determined the region of formulations for SC of the “GBFS – BP – SC – CAA” composition, suitable for use in concrete. The SC formulations were optimized according to the simplex plan of the experiment.

Taking into consideration our results (Fig. 10), we accepted for the studied SC the ratio BP:CAA=1.13 to be a constant.

The following variable factors were adopted: X₁ – the content of GBFS in the composition of SC, 66...100 %; X₂ – the content of PC in the SC composition, 0.0...34.0 %; X₃ – the total content of BP and CAA in the SC composition, 0.0...26.0 %.

The following starting criterion were selected: the molar ratio of Cl⁻/OH⁻ on day 2 and 28 of hardening; the compression strength of SC on day 2, 7, and 28 of hardening.

Based on the optimization results, we have determined the optimal region of SC of the “GBFS – BP – SC – CAA” composition (shaded) (Fig. 13). The specified region is defined by the boundaries given in Table 6.

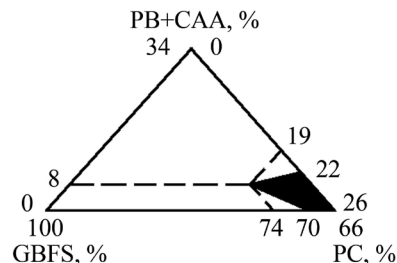


Fig. 13. The region of SC compositions recommended for reinforced concrete

The SC within the optimized composition region is characterized by strength class 42.5 according to EN 197-1 while providing for a molar ratio of Cl⁻/OH⁻ within 0.6.

To study patterns in the structure formation of SC of the “GBFS – BP – SC – CAA” composition, the methods of physical-chemical analysis was used to select a composition from the specified optimal region of formulations, %: GBFS – 66, PC – 26, BP – 4.2, CAA – 3.8.

Table 6

SC formulation for use in reinforced concrete	
SC component, %	Content, %
GBFS	66.0–70.0
PC	22.0–26.0
BP	not exceeding 4.2
CAA	not exceeding 3.8

The resulting correlation between GBFS and PC matches, in accordance with DSTU B V.2.7-46, the slag Portland cement SPC III/B. However, uncertainty about the exact content of GBFS and PC due to significant variation does not make it possible to use SPC III/B as an SC ingredient. In addition, there is a risk of unwanted changes in the morphology and destabilization of hydrate phases, which is associated with the removal of gypsum from the process of cement structure formation during the initial hydration period as a result of exchanging reactions with compounds of alkaline metals [66].

According to the results from DTA (Fig. 14, curve 1), the products of SC hydration on day 2 of hardening are represented by the same new formations as the SC of the “GBFS – BP – PC” composition. The patterns of structure formation include the increased crystallization degree of low-base calcium hydrosilicates CSH(I), which is confirmed by shifting the endoeffects ($t=175$ and 320 °C) and exoeffect ($t=865$ °C) towards the region of high temperatures. In addition, we have observed an increase in the degree of crystallization of calcium hydrosilicates of the structure $C_2SH(A)$, as evidenced by the displacement of endoeffects from 420 to 430 °C and from 480 to 490 °C. This effect causes an increase in the strength of artificial stone when introducing CAA to the SC composition.

The *AFm* phases, identified in the hydration products in the form of Friedel salt and calcium hydrosulfoaluminate, are also characterized by the increased degree of crystallization after 48 hours of hardening when adding a CAA admixture. This is confirmed by the displacement of the endoeffect ($t=175$ °C) and exoeffects ($t=745$ °C and 800 °C, respectively).

Over 28 days of hardening there is a natural increase in the degree of crystallization of the identified hydrate new formations, which is registered by the displacement of the corresponding endoeffects and exoeffects towards the region of elevated temperatures (Fig. 14, curve 2).

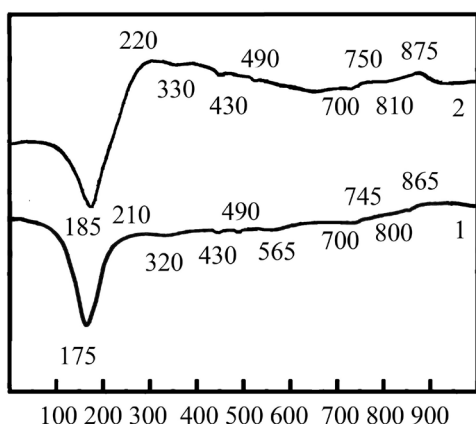


Fig. 14. The curves acquired from a differential-thermal analysis of SC of the “GBFS – BP – PC – CAA” composition: 1 – on day 2 of hardening; 2 – on day 28 of hardening

Portlandite $Ca(OH)_2$, identified on day 2 of hardening (endoeffect at $t=565$ °C) (Fig. 14, curve 1), is not observed in the hardening products on day 28 (Fig. 14, curve 2). This indicates a complete binding of portlandite into other hydration products: hydrosilicates CSH(I), $C_2SH(A)$, and *AFm* phases.

Electron microphotographs of the stone chip’s surface and the data from a probe analysis during hardening complement the results from DTA. Thus, on day 2 of hardening, the formation of Friedel salt was registered (content, %: $CaO - 36.47$, $Al_2O_3 - 19.25$, $Cl - 20.76$) and calcium hydrosulfoaluminate (content, %: $CaO - 39.11$, $Al_2O_3 - 16.83$, $Cl - 17.55$) (Fig. 15, *a, b*) in the form of conglomerates from hexagonal plates, indicating the greater content and degree of crystallization of new formations when adding CAA to SC.

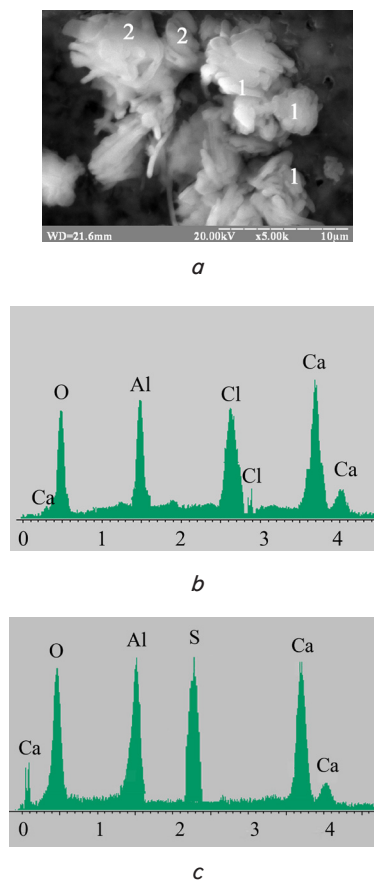


Fig. 15. Characteristics of the microstructure of SC of the “GBFS – BP – PC – CAA” composition after 2 days of hardening: *a* – an electron microphotograph of the chip’s surface; *b, c* – a probe analysis of the new formations, marked 1 and 2, respectively

On day 28, we observed in the products of hydration of SC of the “GBFS – BP – PC – CAA” composition the crystallization of Friedel salt (content, %: $CaO - 38.65$, $Al_2O_3 - 17.37$, $Cl - 22.18$) and calcium hydrosulfoaluminate (content, %: $CaO - 34.12$, $Al_2O_3 - 18.44$, $Cl - 17.58$). This is confirmed by the presence of crystals in the form of hexagonal plates of much larger size compared to that on day 2 (Fig. 16, *a, b*). Our results demonstrate the intensification of the formation of *AFm* phases when introducing CAA into the SC composition.

The established patterns of the structure formation of SC with the optimized composition predetermine the formation of properties necessary for use in steel-reinforced concrete. The required strength is ensured by forming calcium hydrosilicates (CSH(I), $C_2SH(A)$) with a high degree of crystallization in the products of hydration. The content of free chloride- and sulfate-ions is minimized in the porous mortar of

hydrated SC in order to prevent corrosion of reinforcement in concrete due to its effective binding by *AFm* phases, whose formation intensity is predetermined by the introduction of CAA into cement composition.

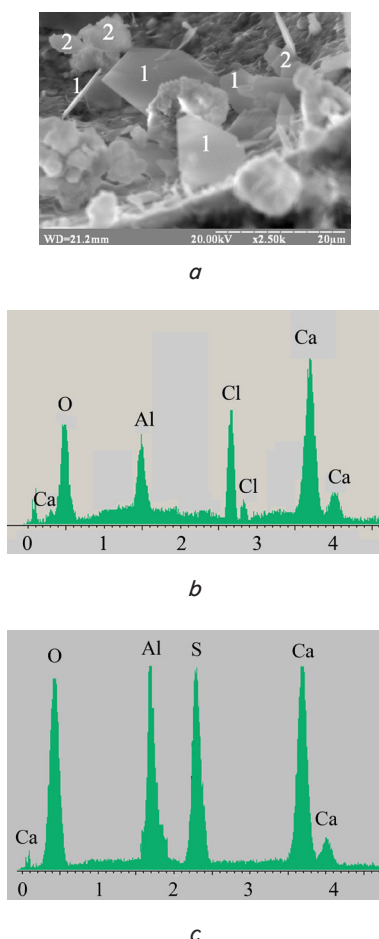


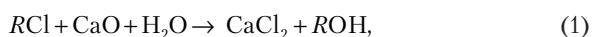
Fig. 16. Characteristics of the microstructure of SC of the “GBFS – BP – PC – CAA” composition after 28 days of hardening: *a* – an electron microphotograph of the chip’s surface; *b, c* – a probe analysis of the new formations, marked 1 and 2, respectively

6. Discussing the study results of devising the slag cement activated by Na(K) salts of strong acids

The study result has made it possible to produce the slag cement activated by SSA, characterized by strength class 42.5 and a value of Cl⁻/OH⁻ in a porous mortar within 0.6. The resulting properties predetermine the possibility of using such SC in steel-reinforced concrete.

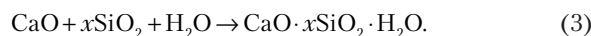
The formation of the specified characteristics is due to the compatible influence of the modifying admixtures of BP, PC, and CAA on the SC structure formation.

The hydraulic properties of GBFS are activated under the influence of strong alkali NaOH formed from an exchange reaction [27]:

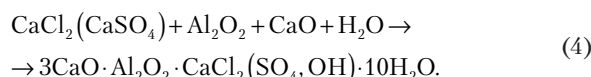


where *R* is an alkaline metal ion (Na⁺, K⁺).

The alkali is involved in the destruction of the slag glass, thereby forming at the surface of the GBFS particles a thin gel-like layer, which consists of silicic acid. As a result of the interaction of the calcium component of the slag with silicic acid, calcium hydrosilicates are formed, which provided for the strength properties of artificial stone [10]:



The chlorides and calcium sulfates, formed from exchange reaction (1), are bound in the low-soluble *AFm* phases (3CaO·Al₂O₃·CaCl₂(SO₄, OH)·10H₂O) [27]:



However, potassium chlorides and potassium sulfates in the BP composition are not fully involved in the formation of *AFm* phases, remaining in the form of ballast. The insufficient activation of GBFS in combination with the presence of the excess content of SSA determines the insufficient strength of SC of the system “GBFS – BP”. This predetermines the feasibility of using additional modifying admixtures in the form of PC and CAA in the SC composition.

Modifying SC with a PC admixture makes it possible to enhance the activating effect of SSA on the slag component (calcium activation). Activating the aluminosilicate glass-like component of GBFS using Ca(OH)₂, which is a product of the Portland cement hydration, contributes to the intensification of formation in the composition of the hydration products of SC of calcium hydrosilicates in the form of CSH(I) and C₂SH(A). Increasing the degree of crystallization of hydrosilicates as part of the hydration products predetermines a significant increase in the strength of artificial stone.

In addition, the indicator that defines the suitability of using SC in reinforced concrete is the content of free chlorine in the porous mortar of cement. A value of this indicator depends on the content of chloride in the BP composition, which is reflected in the development of SC structure formation.

Thus, in the initial period of SC hydration prior to the crystallization of portlandite, there is the following reaction:

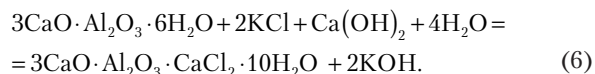


The onset of this process is determined by the dissolution of KCl in the BP composition. CaCl₂ calcium chloride forms with portlandite Ca(OH)₂ a complex compound Ca(OH)₂·x·CaCl₂·2H₂O while the alkaline metal ions increase the pH of the porous solution. During hydration, there is a surface dissolution of Ca(OH)₂·CaCl₂·2H₂O due to the less solubility of portlandite compared to calcium chloride. As a result, there is the crystallization of portlandite and the migration of chlorine ions into a porous solution.

The increased content of potassium chloride in the BP composition causes too high a molar ratio of Cl⁻/OH⁻ in a porous solution, 9.83. However, it is known that the absence of conditions for reinforcement passivation is ensured at the values of the specified indicator not exceeding 0.6.

In order to reduce the content of free chlorine in the SC porous mortar, we propose the introduction of CAA admix-

ture in the form hexahydrated tricalcium calcium aluminate $C_3A \cdot 6H_2O$ $C_3A \cdot 6H_2O$. Modifying SC using CAA leads to the binding of free chlorine into the low-soluble *AFm* phase in the form of Friedel salt according to the following scheme:



Consequently, the role of CAA is to intensify the formation of Friedel salt. It is shown that the kinetic of the formation of Friedel salt is determined by the intensity of the portlandite crystallization process and its subsequent transition into calcite. Under the conditions of carbonization, the re-crystallization of $3CaO \cdot Al_2O_3 \cdot CaCl_2 \cdot 10H_2O$ into $3CaO \cdot Al_2O_3 \cdot 0.5Ca(OH)_2 \cdot 0.5CaCO_3 \cdot 10H_2O$ is possible. It is also possible to replace the $[Cl \cdot 2H_2O]^-$ anions with $[OH \cdot 3H_2O]^-$ in the already created Friedel salt [27].

Thus, the discrepancy between the kinetics of portlandite crystallization (~3 hours) and Friedel salt (4–5 days) determines the role of CAA in the intensification of the formation of the *AFm* phase at the initial stage of SC structure formation.

As a solution to counteract the slow formation of Friedel salt under the influence of carbon dioxide, the use of SAS is proposed as additives that contribute to the compaction of the material's structure.

Thus, a practical component of our study is the increased hydration activity of SC when using BP as a structure-forming component, which is a large-ton byproduct of cement production, as a source of SSA. Effective disposal of industrial by-products (GBFS, BP) with a reduction of CO_2 emission in cement production matches the concept of sustainable development.

The SSA-activated SC, produced as a result of our study, could be used as a base of steel-reinforced concrete. The prospects for this type of GBFS activation and its advantages compared to purely alkali activation are given in work [27]. Thus, the use of SSA as GBFS activators provides for a decrease in the alkalinity of the binder, the minimization of risks of handling high-alkaline materials, as well as the manufacturability of cement. A special feature of the proposed type of activation, implemented in this work, is to use the industrial waste BP as an activator to be a source of SSA, as opposed to chemical compounds [27]. This approach corresponds to the modern trends in the development of the construction industry in terms of responsible attitude to the environment by recycling industrial waste.

However, despite the intensifying effect of the action, the excess content of the anionic component of SSA as part of the SC hydration products could contribute to the evolution of corrosion of steel reinforcement in concrete. Thus, the SC of the system "GBFS – BP – PC", whose content of BP is 17.5 %, is characterized by the maximum compression strength indicators of 9.6 and 29.1 MPa on day 2 and 28, respectively. However, the ratio of Cl^-/OH^- in the porous mortar of the hydrated SC of this composition is 9.83. In this case, the absence of conditions for reinforcement depassivation is ensured when a value of the ratio is $Cl^-/OH^- \leq 0.6$. This circumstance predetermines a decrease in the content of BP in the SC composition and requires the introduction of an additional modifying component – CAA. This limitation was taken into consideration when preparing the optimal composition of SC using mathematical methods to plan the experiment. The resulting SC composition with the content

of BP reduced to 4.2 % is characterized by properties suitable for steel-reinforced concrete.

Our study has not addressed preventing the slow formation of Friedel salt under the influence of CO_2 by compacting the structure of the material when using SAS performing a water-reducing function. This predetermines the prospects for further research into the choice of an effective SAS for concrete based on the devised SC. The relevance of this research area is due to the loss of efficiency by most SAS in the hydration environment of alkali-activated binding systems. Undertaking research in the proposed area would advance those studies that propose the principles of reasonable choice of SAS for different functional purposes (plasticizers [21], redispersing polymeric powders [22], etc.) for alkaline-activated systems.

Another promising field to advance our study is the search for and approbation of other industrial waste and by-products, which are the source of SSA, and are suitable for activating SC.

7. Conclusions

1. We have proven the activating influence of SSA in the BP composition on the hydraulic properties of GBFS, due to the influence of strong alkali NaOH formed from an exchange reaction involving calcium at a content of BP about 30.0 %. It is determined that the hardening of SC is accompanied by the formation in the composition of hydration products of low-base calcium hydrosilicates of the structure CSH(I), the *AFm* phases (Friedel salt $3CaO \cdot Al_2O_3 \cdot CaCl_2 \cdot 10H_2O$, calcium hydrosulfoaluminate $3CaO \cdot Al_2O_3 \cdot CaSO_4 \cdot 12H_2O$) of free portlandite $Ca(OH)_2$. The low strength of SC (16.5 MPa) is due to the insufficient activity of the slag component of cement and the excess content of soluble salts (arcanite K_2SO_4 , sylvite KCl) in the composition of hydration products.

2. It was found that modifying slag cement by an additional component in the form of the Portland cement leads to a significant increase in strength due to the formation of hydrosilicates (CSH(I), $C_2SH(A)$) in the hydration products' composition with an increased degree of crystallization. It is shown that the greatest strength of SC of the system "GBFS – BP – PC" is provided at a PC content of 13.5 % and corresponds to class 32.5. The defined ratio of Cl^-/OH^- in the porous mortar of hydrated SC (9.83) predetermines the evolution of the process of depassivating the steel reinforcement in concrete.

3. The role of CAA in the intensification of binding the anions of strong acid salts (Cl^- , SO_4^{2-}) into *AFm* phases in the composition of hydration products has been confirmed. We have shown an increase in the content and degree of crystallization of the *AFm* phases (Friedel salt, calcium hydrosulfoaluminate) when adding CAA to the SC composition. The slowing effect of CO_2 from the air on the process of formation of Friedel salt has been established, which predetermines the relevance of taking measures to compact the structure of the material through the use of SAS additives.

4. Mathematical methods to plan the experiment were applied to establish the optimal formulation of SC activated by SSA when using BP, PC, and CAA. The optimized SC compositions are characterized by strength class 42.5 and the $Cl^-/OH^- < 0.6$ ratio in a porous mortar, predetermining their suitability for use as a base for steel-reinforced concrete.

Acknowledgments

We express gratitude for the financial support to our work carried out within the State budget funding No. 1020U001010, as well as for advancing research based

on the scientific cooperation program COST Action CA15202 SARCOS “Self-Healing concrete: the path to sustainable construction” within the framework of the European project HORIZON 2020, http://www.cost.eu/COST_Actions/ca/CA15202.

References

1. Abyzov, V. A., Pushkarova, K. K., Kochevykh, M. O., Honchar, O. A., Bazeliuk, N. L. (2020). Innovative building materials in creation an architectural environment. IOP Conference Series: Materials Science and Engineering, 907, 012035. doi: <https://doi.org/10.1088/1757-899x/907/1/012035>
2. Anopko, D. V., Honchar, O. A., Kochevykh, M. O., Kushnierova, L. O. (2020). Radiation protective properties of fine-grained concretes and their radiation resistance. IOP Conference Series: Materials Science and Engineering, 907, 012031. doi: <https://doi.org/10.1088/1757-899x/907/1/012031>
3. Krivenko, P., Petropavlovskiy, O., Kovalchuk, O., Rudenko, I., Konstantynovskiy, O. (2020). Enhancement of alkali-activated slag cement concretes crack resistance for mitigation of steel reinforcement corrosion. E3S Web of Conferences, 166, 06001. doi: <https://doi.org/10.1051/e3sconf/202016606001>
4. Sanytsky, M., Kropyvnytska, T., Fic, S., Ivashchysyn, H. (2020). Sustainable low-carbon binders and concretes. E3S Web of Conferences, 166, 06007. doi: <https://doi.org/10.1051/e3sconf/202016606007>
5. Kropyvnytska, T., Rucinska, T., Ivashchysyn, H., Kotiv, R. (2020). Development of Eco-Efficient Composite Cements with High Early Strength. Lecture Notes in Civil Engineering, 211–218. doi: https://doi.org/10.1007/978-3-030-27011-7_27
6. Markiv, T., Sobol, K., Petrovska, N., Hunyak, O. (2020). The Effect of Porous Pozzolan Polydisperse Mineral Components on Properties of Concrete. Lecture Notes in Civil Engineering, 275–282. doi: https://doi.org/10.1007/978-3-030-27011-7_35
7. Markiv, T., Sobol, K., Franus, M., Franus, W. (2016). Mechanical and durability properties of concretes incorporating natural zeolite. Archives of Civil and Mechanical Engineering, 16 (4), 554–562. doi: <https://doi.org/10.1016/j.acme.2016.03.013>
8. Chepurna, S., Borziak, O., Zubenko, S. (2019). Concretes, Modified by the Addition of High-Diffused Chalk, for Small Architectural Forms. Materials Science Forum, 968, 82–88. doi: <https://doi.org/10.4028/www.scientific.net/msf.968.82>
9. Moskalenko, O., Runova, R. (2016). Ice Formation as an Indicator of Frost-Resistance on the Concrete Containing Slag Cement in Conditions of Freezing and Thawing. Materials Science Forum, 865, 145–150. doi: <https://doi.org/10.4028/www.scientific.net/msf.865.145>
10. Krivenko, P. (2017). Why Alkaline Activation – 60 Years of the Theory and Practice of Alkali-Activated Materials. Journal of Ceramic Science and Technology, 8 (3), 323–334. doi: <https://doi.org/10.4416/JCST2017-00042>
11. Berdnyk, O. Y., Lastivka, O. V., Maystrenko, A. A., Amelina, N. O. (2020). Processes of structure formation and neoformation of basalt fiber in an alkaline environment. IOP Conference Series: Materials Science and Engineering, 907, 012036. doi: <https://doi.org/10.1088/1757-899x/907/1/012036>
12. Pavel, K., Oleg, P., Hryhorii, V., Serhii, L. (2017). The Development of Alkali-activated Cement Mixtures for Fast Rehabilitation and Strengthening of Concrete Structures. Procedia Engineering, 195, 142–146. doi: <https://doi.org/10.1016/j.proeng.2017.04.536>
13. Panias, D., Balomenos, E., Sakkas, K. (2015). The fire resistance of alkali-activated cement-based concrete binders. Handbook of Alkali-Activated Cements, Mortars and Concretes, 423–461. doi: <https://doi.org/10.1533/9781782422884.3.423>
14. Kovalchuk, O., Grabovchak, V., Govdun, Y. (2018). Alkali activated cements mix design for concretes application in high corrosive conditions. MATEC Web of Conferences, 230, 03007. doi: <https://doi.org/10.1051/mateconf/201823003007>
15. Kryvenko, P., Guzii, S., Kovalchuk, O., Kyrychok, V. (2016). Sulfate Resistance of Alkali Activated Cements. Materials Science Forum, 865, 95–106. doi: <https://doi.org/10.4028/www.scientific.net/msf.865.95>
16. Cyr, M., Pouhet, R. (2015). The frost resistance of alkali-activated cement-based binders. Handbook of Alkali-Activated Cements, Mortars and Concretes, 293–318. doi: <https://doi.org/10.1533/9781782422884.3.293>
17. Savchuk, Y., Plugin, A., Lyuty, V., Pluhin, O., Borziak, O. (2018). Study of influence of the alkaline component on the physico-mechanical properties of the low clinker and clinkerless waterproof compositions. MATEC Web of Conferences, 230, 03018. doi: <https://doi.org/10.1051/mateconf/201823003018>
18. Gots, V. I., Gelevera, A. G., Petropavlovsky, O. N., Rogozina, N. V., Smeshko, V. V. (2020). Influence of whitening additives on the properties of decorative slag-alkaline cements. IOP Conference Series: Materials Science and Engineering, 907, 012033. doi: <https://doi.org/10.1088/1757-899x/907/1/012033>
19. Kryvenko, P., Hailin, C., Petropavlovskiy, O., Weng, L., Kovalchuk, O. (2016). Applicability of alkali-activated cement for immobilization of low-level radioactive waste in ion-exchange resins. Eastern-European Journal of Enterprise Technologies, 1 (6 (79)), 40–45. doi: <https://doi.org/10.15587/1729-4061.2016.59489>
20. Kochetov, G., Prikhna, T., Kovalchuk, O., Samchenko, D. (2018). Research of the treatment of depleted nickel-plating electrolytes by the ferritization method. Eastern-European Journal of Enterprise Technologies, 3 (6 (93)), 52–60. doi: <https://doi.org/10.15587/1729-4061.2018.133797>

21. Runova, R., Gots, V., Rudenko, I., Konstantynovskiy, O., Lastivka, O. (2018). The efficiency of plasticizing surfactants in alkali-activated cement mortars and concretes. *MATEC Web of Conferences*, 230, 03016. doi: <https://doi.org/10.1051/mateconf/201823003016>
22. Rudenko, I. I., Konstantynovskiy, O. P., Kovalchuk, A. V., Nikolainko, M. V., Obremsky, D. V. (2018). Efficiency of Redispersible Polymer Powders in Mortars for Anchoring Application Based on Alkali Activated Portland Cements. *Key Engineering Materials*, 761, 27–30. doi: <https://doi.org/10.4028/www.scientific.net/kem.761.27>
23. Krivenko, P. V., Rudenko, I. I., Petropavlovskiy, O. M., Konstantynovskiy, O. P., Kovalchuk, A. V. (2019). Alkali-activated Portland cement with adjustable proper deformations for anchoring application. *IOP Conference Series: Materials Science and Engineering*, 708, 012090. doi: <https://doi.org/10.1088/1757-899x/708/1/012090>
24. Krivenko, P. V., Petropavlovskiy, O. M., Rudenko, I. I., Konstantynovskiy, O. P., Kovalchuk, A. V. (2020). Complex multifunctional additive for anchoring grout based on alkali-activated portland cement. *IOP Conference Series: Materials Science and Engineering*, 907, 012055. doi: <https://doi.org/10.1088/1757-899x/907/1/012055>
25. Kropyvnytska, T. P., Kaminsky, A. T., Semeniv, R. M., Chekaylo, M. V. (2019). The effect of sodium aluminate on the properties of the composite cements. *IOP Conference Series: Materials Science and Engineering*, 708, 012091. doi: <https://doi.org/10.1088/1757-899x/708/1/012091>
26. Bai, Y., Collier, N. C., Milestone, N. B., Yang, C. H. (2011). The potential for using slags activated with near neutral salts as immobilisation matrices for nuclear wastes containing reactive metals. *Journal of Nuclear Materials*, 413 (3), 183–192. doi: <https://doi.org/10.1016/j.jnucmat.2011.04.011>
27. Bernal, S. A. (2016). Advances in near-neutral salts activation of blast furnace slags. *RILEM Technical Letters*, 1, 39. doi: <https://doi.org/10.21809/rilemtechlett.v1.8>
28. Mobasher, N., Bernal, S. A., Hussain, O. H., Apperley, D. C., Kinoshita, H., Provis, J. L. (2014). Characterisation of $\text{Ba}(\text{OH})_2$ – Na_2SO_4 –blast furnace slag cement-like composites for the immobilisation of sulfate bearing nuclear wastes. *Cement and Concrete Research*, 66, 64–74. doi: <https://doi.org/10.1016/j.cemconres.2014.07.006>
29. Mobasher, N., Bernal, S. A., Provis, J. L. (2016). Structural evolution of an alkali sulfate activated slag cement. *Journal of Nuclear Materials*, 468, 97–104. doi: <https://doi.org/10.1016/j.jnucmat.2015.11.016>
30. Krivenko, P., Sanytsky, M., Kropyvnytska, T. (2018). Alkali-Sulfate Activated Blended Portland Cements. *Solid State Phenomena*, 276, 9–14. doi: <https://doi.org/10.4028/www.scientific.net/ssp.276.9>
31. Bilek, V., Kalina, L., Simonova, H. (2019). Effect of curing environment on length changes of alkali-activated slag/cement kiln by-pass dust mixtures. *IOP Conference Series: Materials Science and Engineering*, 583, 012017. doi: <https://doi.org/10.1088/1757-899x/583/1/012017>
32. Maslehuddin, M., Al-Amoudi, O. S. B., Shameem, M., Rehman, M. K., Ibrahim, M. (2008). Usage of cement kiln dust in cement products – Research review and preliminary investigations. *Construction and Building Materials*, 22 (12), 2369–2375. doi: <https://doi.org/10.1016/j.conbuildmat.2007.09.005>
33. Bilek Jr., V., Kalina, L., Bartoničková, E., Opravil, T. (2014). Influence of Industrial By-Products on Shrinkage of Alkali-Activated Slag. *Advanced Materials Research*, 1000, 137–140. doi: <https://doi.org/10.4028/www.scientific.net/amr.1000.137>
34. Krivenko, P. V., Petropavlovskiy, O., Rudenko, I., Konstantynovskiy, O. P. (2019). The Influence of Complex Additive on Strength and Proper Deformations of Alkali-Activated Slag Cements. *Materials Science Forum*, 968, 13–19. doi: <https://doi.org/10.4028/www.scientific.net/msf.968.13>
35. Collier, N. C., Li, X., Bai, Y., Milestone, N. B. (2015). The effect of sulfate activation on the early age hydration of BFS:PC composite cement. *Journal of Nuclear Materials*, 464, 128–134. doi: <https://doi.org/10.1016/j.jnucmat.2015.04.044>
36. Aliabdo, A. A., Abd Elmoaty, A. E. M., Emam, M. A. (2019). Factors affecting the mechanical properties of alkali activated ground granulated blast furnace slag concrete. *Construction and Building Materials*, 197, 339–355. doi: <https://doi.org/10.1016/j.conbuildmat.2018.11.086>
37. Bilek Jr., V., Pařízek, L., Kosár, P., Kratochvíl, J., Kalina, L. (2016). Strength and Porosity of Materials on the Basis of Blast Furnace Slag Activated by Liquid Sodium Silicate. *Materials Science Forum*, 851, 45–50. doi: <https://doi.org/10.4028/www.scientific.net/msf.851.45>
38. Criado, M. (2015). The corrosion behaviour of reinforced steel embedded in alkali-activated mortar. *Handbook of Alkali-Activated Cements, Mortars and Concretes*, 333–372. doi: <https://doi.org/10.1533/9781782422884.3.333>
39. Buchwald, A., Schulz, M. (2005). Alkali-activated binders by use of industrial by-products. *Cement and Concrete Research*, 35 (5), 968–973. doi: <https://doi.org/10.1016/j.cemconres.2004.06.019>
40. Bernal, S. A., Ke, X., Provis, J. L. (2015). Activation of slags using near-neutral salts: The importance of the slag chemistry. 14th International Congress on Chemistry of Cement. Beijing.
41. Krivenko, P., Gots, V., Petropavlovskiy, O., Rudenko, I., Konstantynovskiy, O., Kovalchuk, A. (2019). Development of solutions concerning regulation of proper deformations in alkali-activated cements. *Eastern-European Journal of Enterprise Technologies*, 5 (6 (101)), 24–32. doi: <https://doi.org/10.15587/1729-4061.2019.181150>
42. Rashad, A. M., Bai, Y., Basheer, P. A. M., Milestone, N. B., Collier, N. C. (2013). Hydration and properties of sodium sulfate activated slag. *Cement and Concrete Composites*, 37, 20–29. doi: <https://doi.org/10.1016/j.cemconcomp.2012.12.010>

43. Wu, P., Wang, J., Lian, M., Lyu, X. (2019). Preparation of slag based cementitious material and its application in the cementation of tailings. In IMPC 2018 - 29th International Mineral Processing Congress, 3122–3137.
44. Rashad, A. M., Bai, Y., Basheer, P. A. M., Collier, N. C., Milestone, N. B. (2012). Chemical and mechanical stability of sodium sulfate activated slag after exposure to elevated temperature. *Cement and Concrete Research*, 42 (2), 333–343. doi: <https://doi.org/10.1016/j.cemconres.2011.10.007>
45. Mobasher, N., Kinoshita, H., Bernal, S. A., Sharrard, C. A. (2014). Ba(OH)₂- blast furnace slag composite binders for encapsulation of sulphate bearing nuclear waste. *Advances in Applied Ceramics*, 113 (8), 460–465. doi: <https://doi.org/10.1179/1743676114y.00000000148>
46. Omelchuk, V., Ye, G., Runova, R., Rudenko, I. I. (2018). Shrinkage Behavior of Alkali-Activated Slag Cement Pastes. *Key Engineering Materials*, 761, 45–48. doi: <https://doi.org/10.4028/www.scientific.net/kem.761.45>
47. Khan, M. S. H., Kayali, O. (2016). Chloride binding ability and the onset corrosion threat on alkali-activated GGBFS and binary blend pastes. *European Journal of Environmental and Civil Engineering*, 22 (8), 1023–1039. doi: <https://doi.org/10.1080/19648189.2016.1230522>
48. Maes, M., Gruyaert, E., De Belie, N. (2012). Resistance of concrete with blast-furnace slag against chlorides, investigated by comparing chloride profiles after migration and diffusion. *Materials and Structures*, 46 (1-2), 89–103. doi: <https://doi.org/10.1617/s11527-012-9885-3>
49. De Weerd, K., Orsáková, D., Geiker, M. R. (2014). The impact of sulphate and magnesium on chloride binding in Portland cement paste. *Cement and Concrete Research*, 65, 30–40. doi: <https://doi.org/10.1016/j.cemconres.2014.07.007>
50. Clark, B. A., Brown, P. W. (2000). The formation of calcium sulfoaluminate hydrate compounds: Part II. *Cement and Concrete Research*, 30 (2), 233–240. doi: [https://doi.org/10.1016/s0008-8846\(99\)00234-3](https://doi.org/10.1016/s0008-8846(99)00234-3)
51. Runci, A., Serdar, M., Provis, J. (2019). Chloride-induced corrosion of steel embedded in alkali-activated materials: state of the art. 5th Symposium on Doctoral Studies in Civil Engineering, 175–185. doi: <https://doi.org/10.5592/co/phdsym.2019.15>
52. Ye, H., Huang, L., Chen, Z. (2019). Influence of activator composition on the chloride binding capacity of alkali-activated slag. *Cement and Concrete Composites*, 104, 103368. doi: <https://doi.org/10.1016/j.cemconcomp.2019.103368>
53. Honorio, T., Guerra, P., Bourdot, A. (2020). Molecular simulation of the structure and elastic properties of ettringite and monosulfoaluminate. *Cement and Concrete Research*, 135, 106126. doi: <https://doi.org/10.1016/j.cemconres.2020.106126>
54. Baquerizo, L. G., Matschei, T., Scrivener, K. L., Saeidpour, M., Wadsö, L. (2015). Hydration states of AFm cement phases. *Cement and Concrete Research*, 73, 143–157. doi: <https://doi.org/10.1016/j.cemconres.2015.02.011>
55. Plugin, A. A., Borziak, O. S., Pluhin, O. A., Kostuk, T. A., Plugin, D. A. (2020). Hydration Products that Provide Water-Repellency for Portland Cement-Based Waterproofing Compositions and Their Identification by Physical and Chemical Methods. *Proceedings of EcoComfort 2020. Lecture Notes in Civil Engineering*, 328–335. doi: https://doi.org/10.1007/978-3-030-57340-9_40
56. Babae, M., Castel, A. (2018). Chloride diffusivity, chloride threshold, and corrosion initiation in reinforced alkali-activated mortars: Role of calcium, alkali, and silicate content. *Cement and Concrete Research*, 111, 56–71. doi: <https://doi.org/10.1016/j.cemconres.2018.06.009>
57. Mesbah, A., Cau-dit-Coumes, C., Frizon, F., Leroux, F., Ravaux, J., Renaudin, G. (2011). A New Investigation of the Cl⁻-CO₃²⁻ Substitution in AFm Phases. *Journal of the American Ceramic Society*, 94 (6), 1901–1910. doi: <https://doi.org/10.1111/j.1551-2916.2010.04305.x>
58. Geng, J., Yang, H., Mo, L. (2015). Effect of attack of sodium sulfate solution on the stability of bounded chloride ions. *Jianzhu Cailiao Xuebao/Journal of Building Materials*, 18 (6), 919–925. doi: <https://doi.org/10.3969/j.issn.1007-9629.2015.06.001>
59. Park, J. W., Ann, K. Y., Cho, C.-G. (2015). Resistance of Alkali-Activated Slag Concrete to Chloride-Induced Corrosion. *Advances in Materials Science and Engineering*, 2015, 1–7. doi: <https://doi.org/10.1155/2015/273101>
60. Pushkareva, K. K., Gonchar, O. A., Kaverin, K. O. (2019). The role of the crystallo-chemical factor in the evaluation and improvement of the nanomodification efficiency of mortar and concrete. *IOP Conference Series: Materials Science and Engineering*, 708, 012102. doi: <https://doi.org/10.1088/1757-899x/708/1/012102>
61. Vollpracht, A., Lothenbach, B., Snellings, R., Haufe, J. (2015). The pore solution of blended cements: a review. *Materials and Structures*, 49 (8), 3341–3367. doi: <https://doi.org/10.1617/s11527-015-0724-1>
62. Krivenko, P. V., Guzii, S. G., Bondarenko, O. P. (2019). Alkaline Aluminosilicate Binder-Based Adhesives with Increased Fire Resistance for Structural Timber Elements. *Key Engineering Materials*, 808, 172–176. doi: <https://doi.org/10.4028/www.scientific.net/kem.808.172>
63. Tsapko, Y., Zavalov, D., Bondarenko, O., Marchenco, N., Mazurchuk, S., Horbachova, O. (2019). Determination of thermal and physical characteristics of dead pine wood thermal insulation products. *Eastern-European Journal of Enterprise Technologies*, 4 (10 (100)), 37–43. doi: <https://doi.org/10.15587/1729-4061.2019.175346>
64. Tsapko, Y., Bondarenko, O. P., Tsapko, A. (2019). Research of the Efficiency of the Fire Fighting Roof Composition for Cane. *Materials Science Forum*, 968, 61–67. doi: <https://doi.org/10.4028/www.scientific.net/msf.968.61>
65. Plugin, A. A., Pluhin, O. A., Borziak, O. S., Kaliuzhna, O. V. (2019). The Mechanism of a Penetrative Action for Portland Cement-Based Waterproofing Compositions. *Lecture Notes in Civil Engineering*, 34–41. doi: https://doi.org/10.1007/978-3-030-27011-7_5
66. Krivenko, P., Gots, V., Runova, R., Rudenko, I., Lastivka, O. (2013). Features of Alkali-Activated Slag Portland Cement. 1st Intern. Conf. on the Chemistry of Construction Materials. Berlin, 453–456.